Self-Similarity of Wind-Wave Spectra. Numerical and Theoretical Studies

Sergei I. Badulin[1], Andrei N. Pushkarev[2,3], Donald Resio[4], and Vladimir E. Zakharov[2,5]

[1] P.P.Shirshov Institute of Oceanology, Moscow, Russia
bsi@wave.sio.rssi.ru
[2] Waves and Solitons LLC, Phoenix, Arizona, USA
andrei@cox.net
[3] Landau Institute for Theoretical Physics, Moscow, Russia
[4] Coastal and Hydraulics Laboratory, Massachusets, USA
Donald.T.Resio@erdc.usace.army.mil
[5] University of Arizona, Tucson, USA
zakharov@math.arizona.edu

Abstract. Results of theoretical and numerical studies of the Hasselmann kinetic equation for wind waves are presented. Approximate self-similar solutions for duration-limited and fetch-limited wind-wave growth are analyzed and related with the classic Kolmogorov spectra of the weak turbulence theory. It is shown that these solutions can be considered as non-stationary and non-homogeneous generalization of these spectra. The experimental parameterizations like JONSWAP spectrum, that have features of self-similarity, give a solid basis for comparison with the theoretical predictions. The comparison is detailed in extensive numerical studies of duration-limited growth of wind waves basing on the algorithm by Webb [20] first realized by Resio & Perrie [16]. Strong tendency of numerical solutions to self-similar behaviour is shown for rather wide range of conditions of wave generation and dissipation. A composite model of wind-wave balance is proposed for description of the self-similar fraction of wind-wave field: the shapes of the solutions are described by the "conservative" Hasselmann equation while the wave growth is determined by the balance equation for generation and dissipation in an integral form. The shapes of the self-similar spectra display perfect coincidence with the spectra measured in the JONSWAP and other major fetch-limited studies, while parameters of wave growth governed by the balance equation are consistent with experimental dependencies of total wave energy and mean frequency on time.

1 Introduction

The rogue waves in the ocean do not exist on their own. Their appearance and transformation is closely linked with environmental conditions and, first of all, with the wind-wave state.

Spectral description is widely used to describe the wind-wave field and its evolution in time and space. Experimental parameterizations of the spectra imply

self-similar and quasi-universal dependencies of the spectra on a set of non-dimensional parameters. E.g. the widely used modified JONSWAP spectrum [5, 4] has exactly the form of the so-called incomplete or the second type self-similar dependence

$$E(\omega) = \alpha_T g^2 \omega^{-4} \omega_p^{-1} \exp\left[-\left(\frac{\omega}{\omega_p}\right)^{-4}\right] \gamma^{\exp[-\frac{(\omega-\omega_p)^2}{2\sigma_p^2\omega_p^2}]} \tag{1}$$

where the spectrum shape depends on an "internal" parameter — non-dimensional frequency ω/ω_p, while the dependence of α_T on an "external" parameter — inverse wave age $U_{10}/C_p = \omega_p U_{10}/g$ is generally fitted by power-like approximation [21]

$$\alpha_T = \alpha_0 (U_{10}\omega_p/g)^{\kappa_\alpha} \tag{2}$$

Hereafter C_p and ω_p are phase speed and frequency of the peak component of wave spectra and wind speed U_h is taken at some reference height h. For α_0 we accept the estimate [1]:

$$\alpha_0 = 0.08/(2\pi) \tag{3}$$

The standard set of shape parameters was proposed as a good fit for the JONSWAP data

$$\gamma = 3.3; \tag{4}$$

$$\sigma = \begin{cases} \sigma_a = 0.07 & \text{for} \quad \omega \le \omega_p; \\ \sigma_b = 0.09 & \text{for} \quad \omega > \omega_p \end{cases} \tag{5}$$

Wave spectra at different stages of wave development can differ considerably from the "universal" parameterization (1) with fixed shape parameters (4, 5). Later basing on analysis of various wave data these parameters have been treated as functions of wind-wave conditions, first of all, of wave age.

Probability of rogue waves can show significant correlation with the spectral shapes variability, in particular, with the peakedness parameter γ [7, 12, 13]. Thus, more accurate description and forecasting of wind-wave spectra (not integral or mean characteristics of waves only) may be useful for prediction of rogue wave events.

In this paper we present recent results of theoretical and numerical studies of the Hasselmann kinetic equation that is a basis of many wave prediction models such as WAM and SWAN. This equation describes evolution of spectral densities of wave action $N(\mathbf{k})$ (or energy $E(\mathbf{k})$) as a result of nonlinear transfer due to four-wave resonant interactions and numerous mechanisms of wave generation and dissipation (wind impact, turbulence etc.)

$$\frac{\partial N_\mathbf{k}}{\partial t} + \nabla_\mathbf{k}\omega_\mathbf{k}\nabla_\mathbf{r} N_\mathbf{k} = S_{nl} + S_{in} + S_{diss} \tag{6}$$

While the nonlinear transfer term S_{nl} is known "from the first principles" the knowledge of wave input S_{in} and generation S_{diss} terms is based mainly on experimental parameterizations. The dispersion of wave input terms S_{in} given

by different authors is comparable in magnitude with the terms themselves. This raises the evident question: whether the models can provide a reliable wave forecasting when there is the uncertainty in source functions in (6)?

The message of the study:
The nonlinear transfer is a dominating mechanism of developing wind-wave spectra and, thus, basic features of the spectra evolution can be predicted quite well without knowledge of details of non-conservative terms S_{in} and S_{diss}.

In §2 the theoretical analysis of the asymptotic self-similar solutions of the Hasselmann equation is presented. We show that the self-similar behaviour of wind-wave spectra is a result of the dominating non-linear transfer as compared with wave input and dissipation.

In §3 we consider numerical solutions of the Hasselmann equation for different functions of wave input and find that the self-similar behaviour of these solutions shows universality features, i.e. spectral shapes depend very slightly on parameters of wave input.

In §4 we analyse variations of the numerical solutions from a universal shape and show that these solutions can be presented effectively as a self-similar "core" superimposed on a non-self-similar background. The evolution of the self-similar core depends rather slightly on the particular wave input function S_{in} and, thus, the parameters of the core — the peak frequency and the spectral peak magnitude can be predicted better than mean frequency and total wave energy contaminated by non-self-similar wave background.

In Discussion we propose a composite model of evolution of wind-wave spectra basing on the concept of self-similarity and universality of spectra of wind-driven waves.

2 Self-Similar Solutions for the Hasselmann Equation

The Hasselmann equation [8] is a subject of the theory of weak turbulence. The key point of the theory is investigation of the stationary kinetic equation

$$S_{nl} = 0 \tag{7}$$

The Rayleigh-Jeans solutions describe local balance of each resonant quadruplet of water wave harmonics, while the so-called Kolmogorov-Zakharov (KZ) solutions correspond to a dynamical equilibrium when input and output for each element of the nonlinear system are balanced, i.e. spectral fluxes of integrals of motion are constant. Two solutions of this type play a fundamental role: the direct cascade solution with a constant flux of energy from large to small wave scales [22] and the inverse cascade solution that describes a constant flux of wave action to long waves [23]. These solutions are usually considered as irrelevant to wind-wave problems because they are isotropic and non-localized in wave scales.

A generalization of the KZ solutions can be found for "conservative" non-stationary or non-homogeneous kinetic equations that model duration-limited

$$\frac{\partial N_{\mathbf{k}}}{\partial t} = S_{nl} \tag{8}$$

or fetch-limited growth [24] of wind-driven waves in $x-$direction

$$\frac{\partial \omega}{\partial k_x}\frac{\partial N_{\mathbf{k}}}{\partial x} = S_{nl} \tag{9}$$

Further we shall discuss the duration-limited case only, the fetch-limited case can be analysed similarly. Details can be found in [2, 3]. The models (8, 9) do not contain terms or wave input or dissipation. In fact, sources and sinks are implied at infinitely small and at infinitely large wave scales quite similarly to the constant flux KZ solutions. The homogeneity property of the collision integral

$$S_{nl} \sim N^3 |\mathbf{k}|^{19/2} \tag{10}$$

allows for constructing non-stationary anisotropic self-similar solutions in the form (duration-limited case)

$$N(\boldsymbol{\xi}) = a t^{\alpha} U_{\beta}(\boldsymbol{\xi}) \tag{11}$$

where the self-similar variable $\boldsymbol{\xi} = b\mathbf{k}t^{\beta}$ and the solution parameters obey

$$a = b^{19/4}; \quad \alpha = (19\beta - 2)/4 \tag{12}$$

The exponents α and β can be determined from the condition of power-like growth of total wave action

$$N_{tot} \sim \int N(\boldsymbol{\xi}, t) \mathrm{d}\mathbf{k} \sim b^{11/4} t^{r} \tag{13}$$

As already noted, the self-similar solutions (11) with parameters defined by (12, 13) imply sources (sinks). The integral condition (13) replaces wave input and dissipation term in the generic Hasselmann equation (6). One has for the exponent of wave action growth

$$r = \alpha - 2\beta = (11\beta - 2)/4 = (11\alpha - 4)/19 \tag{14}$$

For the total wave energy $E_{tot} \sim t^p$ one gets

$$p = \alpha - 5\beta/2 = (11\beta - 4)/4 = (9\alpha - 5)/19 \tag{15}$$

The "shape" function $U_{\beta}(\boldsymbol{\xi})$ satisfies the equation in self-similar variables that resembles a stationary kinetic equation with a special source term

$$\alpha U_{\beta} + \beta \boldsymbol{\xi} \nabla_{\boldsymbol{\xi}} U_{\beta} = S_{nl}[U(\boldsymbol{\xi})] \tag{16}$$

In fact, we split the Hasselmann equation into two parts. The first one (16) gives a shape of the solutions, while the condition (13) describes an integral balance of wave action. This composite model of the wind-wave balance implies that the nonlinear transfer dominates as compared with wave input and, thus, the latter

can be taken into account in the integral form (13). A simple estimate of validity of such substitution gives for the duration-limited case

$$\alpha > 1; \qquad r > 7/19 \tag{17}$$

— the solution should grow fast enough for the nonlinearity to be dominating over the wave input and dissipation terms. The result is physically transparent — the strong non-linear transfer requires strong non-stationarity. In fact, the effect of dominating collision integral S_{nl} in the kinetic equation can be justified correctly in numerical experiments only.

3 Quasi-Universality of Wind-Wave Spectra

Extensive numerical studies of the Hasselmann equation (6) for different wave input parameterizations [6, 11, 17, 14, 18] has been carried out recently basing on the Resio & Perrie approach [16] improved by Pushkarev [15]. The analysis of the numerical solutions was focused on features of self-similarity of wind-wave spectra. The form of the approximate self-similar solutions (11) allows for a time-independent presentation of the solution and, thus, for an analysis of dependencies in terms of non-dimensional wave frequencies. Using the freedom in scaling parameters a and b in (12) one can let

$$\boldsymbol{\xi} = b|\mathbf{k}|t^{\beta} = (\omega/\omega_p)^2; \qquad U_\beta(1) = 1 \tag{18}$$

Quite similarly to the parameterizations of wind-wave spectra (e.g. eq.1) one has a form of the second-type self-similar dependence in terms of non-dimensional frequency ("internal" variable) and an "external" combination of the scaling parameters a, b and the solution peak frequency — a straightforward analogue of wind-wave age. These dependencies can be analysed separately in order to check the idea of self-similarity of the numerical solutions.

Two large series of experiments were carried out. First, the "academic" experiments with special input functions in (6) have been targeted at obtaining the self-similarity properties "in pure" state in the wide range of the key parameter of self-similarity r — the exponent of total wave action growth. All the experiments showed very strong tendency of the numerical solutions to the asymptotic self-similar behaviour. Moreover, the "shape" functions $U_\beta(\boldsymbol{\xi})$ (18) for different β (or r) were found to be rather close to each other. In other words, the shapes of the asymptotic solutions turn out to be quasi-universal, independent of input function S_{in}.

The results of the "academic" series have been used as a reference for the second series of numerical experiments with realistic input functions given by experimental parameterizations [6, 11, 17, 14, 18]. The similar strong tendency to self-similar behaviour has been observed in this case and, quite like to the "academic" experiments, the shape functions $U_\beta(\boldsymbol{\xi})$ have been found to be quasi-universal. Fig.1 illustrates this result for parameterizations of input functions by Snyder et al. [17], Hsiao & Shemdin [11] and swell. The normalized dependence

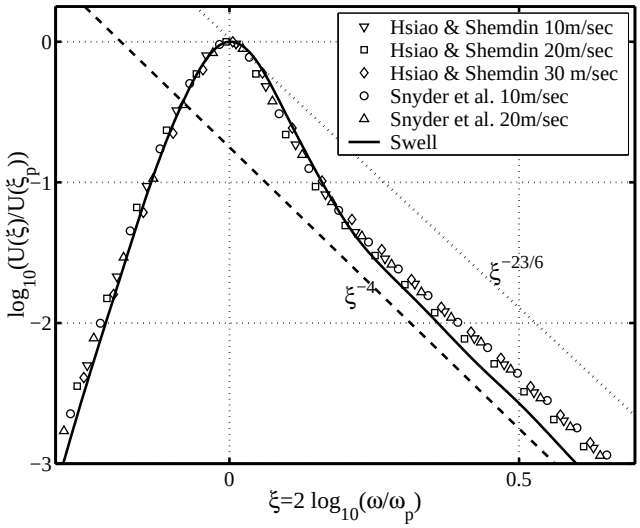

Fig. 1. Normalized spatial spectra of wave action $U_\beta(\boldsymbol{\xi})/U_\beta(\boldsymbol{\xi}_p)$ for down-wind direction as functions of non-dimensional frequency ω/ω_p for different wave input parameterizations and wind speeds (shown in legend). The JONSWAP spectrum for the standard peakedness $\gamma = 3.3$ is shown by dashed curve. Power laws for stationary Kolmogorov's solutions are shown by dashed (ω^{-4} — direct cascade) and dotted lines ($\omega^{-23/6}$ — inverse cascade).

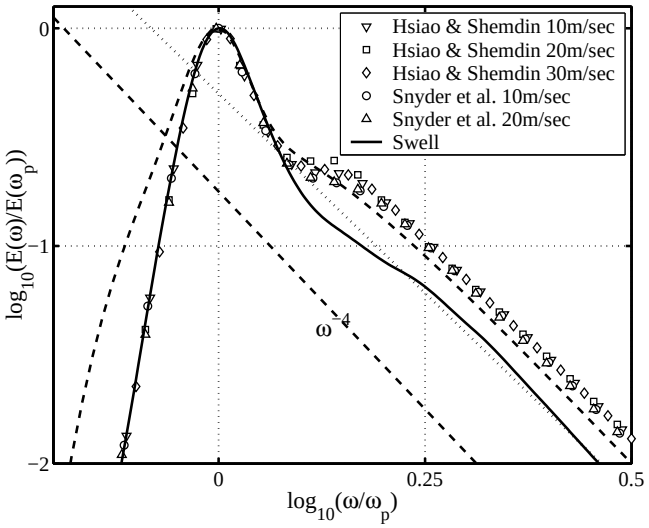

Fig. 2. Normalized frequency spectra $E(\omega)/E(\omega_p)$ as functions of non-dimensional frequency ω/ω_p for different wave input parameterizations and wind speeds (shown in legend). The JONSWAP spectrum for the standard peakedness $\gamma = 3.3$ is shown by dashed curve. Power laws for stationary Kolmogorov's solutions are shown by dashed (ω^{-4} — direct cascade) and dotted lines ($\omega^{-11/3}$ — inverse cascade).

$U_\beta(\boldsymbol{\xi})/U_\beta(\boldsymbol{\xi}_p)$ is shown for down-wind direction where the wave input is maximal. In view of this fact and the results of the "academic" series the universality of the shapes of solutions in self-similar variables does not look surprising as far as the corresponding self-similarity parameter r varied very slightly: in all the experiments with realistic pumping $0.85 < r < 1.0$. The special case of swell ($r \approx 0$, solid curves in figs.1, 2) shows a visible difference as compared to other cases. The difference of numerical solutions for different wave inputs becomes prominent in terms of spectra averaged in direction. Fig.2 shows the normalized frequency spectra for the same set of numerical runs as fig.1. The spectral shapes are close to each other and to the standard JONSWAP dependence (dashed line) near the peak (approximately up to $1.3\omega_p$) and at high-frequency tails ($\omega > 2\omega_p$).

In the range $1.3 < \omega_p < 2\omega_p$ noticeable variations of spectra are observed depending on the wave input parameterization and on time. The relaxation of the solutions to an asymptotic form is very fast irrespectively to the wave input parameterization: generally, it takes less than 2 hours for a solution to fit its asymptotic with accuracy less than 5%. For the range $1.3 < \omega_p < 2\omega_p$ this time is substantially longer. Figs.3, 4 illustrates this result for approximately 2 and 8 hours of development of wave spectrum with the parameterization [6] and wind speed 10 m/s. A plateau is seen in the spectrum at 8 hours (fig.4). In some experiments a prominent peak was observed in the same frequency range. In all the cases the shape of the spectral peak is reproduced remarkably well irrespectively to the way of wave pumping while outside the narrow peak there is a variety of spectral forms that depends on wave pumping and the stage of wind-wave development.

Our analysis of self-similarity features allows to present (at the moment qualitatively) the wind-wave spectra as a combination of a self-similar "core" and a wave background. Evidently, the evolution of the core that does not depend on details of functions S_{in} and S_{diss} can be predicted quite well while the spectrum background depends on these details essentially and, thus, cannot be forecasted reliably.

4 Exponents of Wind-Wave Growth

The next part of our analysis of self-similarity features of the numerical wind-wave spectra concerns the evolution of global properties of wind-wave field such as characteristic frequencies (periods) and total energy (or significant wave height). In view of previous results the question can be formulated as follows: *What characteristics of wind-wave field are more adequate to the problem of wind-wave prediction? What predictions are more reliable?*

The wind-wave growth can be characterized in different ways: first, in terms of mean (integral) quantities like dispersion of wave heights or mean frequency, second, in terms of characteristic quantities of spectral distribution, i.e. peak frequency and spectral peak magnitude. Certainly, the first way is easier to realize, while the latter method requires more keen data processing. In our numerical experiments one can calculate easily both sets of characteristics and the corre-

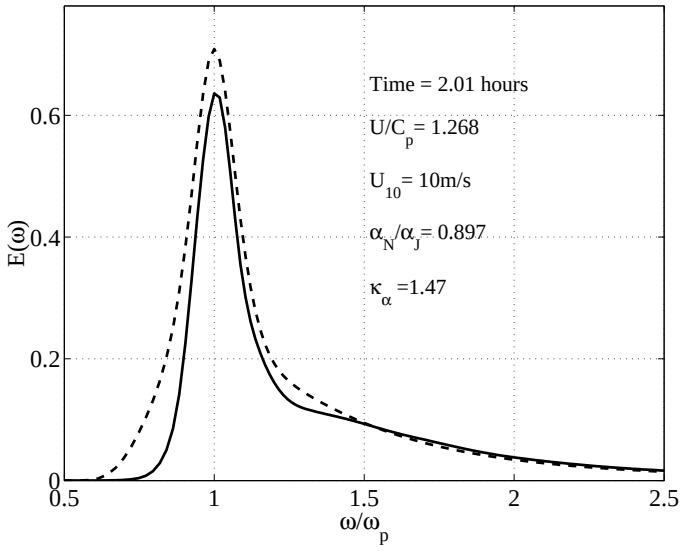

Fig. 3. Frequency spectra for numerical solution of the Hasselmann equation with Donelan et al. wave generation rate [5] (solid line) and modified JONSWAP spectrum (eq.1, dashed) for "young" waves. Wind speed $U_{10} = 10$m/s, time 2 hours

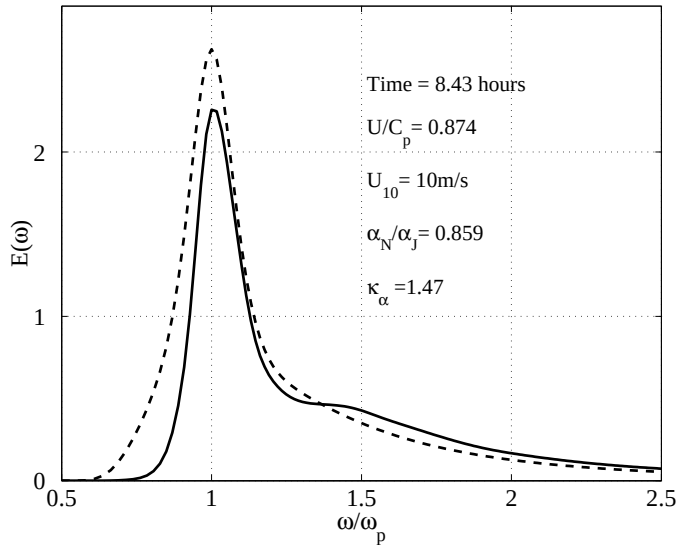

Fig. 4. The same as in previous figure for time approximately 8 hours

sponding exponents of power-like fits. For total energy and mean frequency one can define (see eq.15) these exponents as follows

$$E_{tot} = \int E(\mathbf{k})\mathrm{d}\mathbf{k} \sim t^p; \qquad \omega_{mean} = \frac{\int \omega E(\mathbf{k})\mathrm{d}\mathbf{k}}{E_{tot}} \sim t^{-q} \tag{19}$$

These definitions take into account the wave spectrum globally, that is, in terms of the previous section, both self-similar core and non-self-similar fraction of the spectrum contribute into the exponents p and q.

Alternatively, one can try to extract parameters of the growth of self-similar core of the numerical solutions by tracing dependencies of peak frequency and the spectral peak magnitude. In terms of exponents α and β in (11) one can calculate easily the "self-similar counterparts" of p and q

$$p_{ss} = \alpha - 5\beta/2 = (11\beta - 4)/4 = (9\alpha - 5)/19; \quad q_{ss} = \beta/2 = (2\alpha + 1)/19 \tag{20}$$

The parameter α is more useful for calculating p_{ss} and q_{ss} because of wider

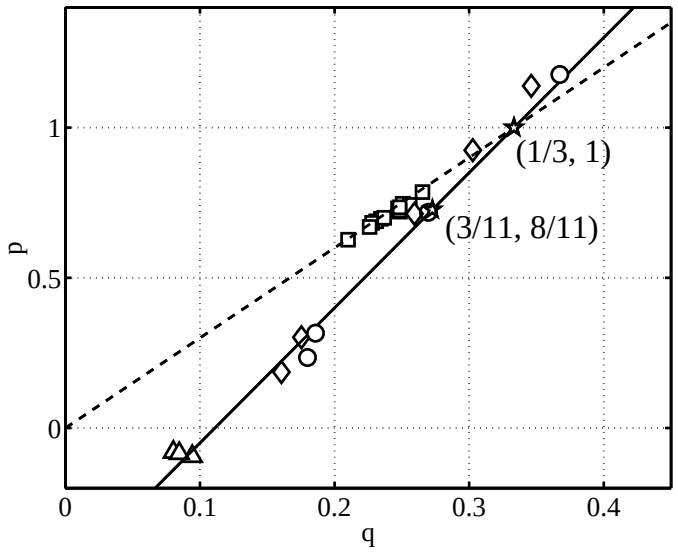

Fig. 5. Exponents p and q for power-like approximations of total energy and mean frequency of the kinetic equation solutions. ◯ — Isotropic 'academic' runs; ◊ — Anisotropic 'academic' runs; △ — Swell; □ — 'Real' wave pumping. Exponents for constant wave action and wave energy inputs are given by stars. Hard line shows theoretical dependence of p on q, dashed line corresponds to Toba's law.

range of change of the spectra magnitudes. The use of β is limited essentially by discrete frequency grid. Introduce the corresponding Toba's parameter

$$T = p/(2q); \qquad T_{ss} = p_{ss}/(2q_{ss}) = \frac{9\alpha - 5}{4\alpha + 2} \tag{21}$$

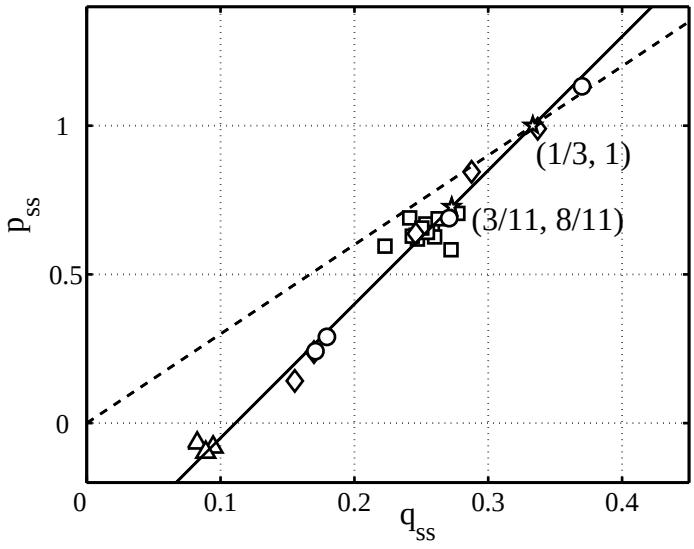

Fig. 6. The same as in previous figure for exponents p_{exp} and q_{exp} calculated for the parameters of solutions' peaks (exponents α and β of the self-similar solutions).

that describes the power-like dependence of significant wave height on wave period (frequency)

$$A \sim (1/\omega)^T$$

The empirical value of the exponent $T = 3/2$ has been obtained by Toba [19]. Fig.5 presents values of exponents of wave growth for different numerical experiments with both "academic" and "realistic" functions of wave input. One can see that "academic" series follow the self-similar relation (20) rather than Toba's law 3/2. At the same time the "realistic" series give the exponents that are closer to Toba's exponent 3/2 (dashed line). This divergence in "academic" and "realistic" dependencies becomes vanishing if we consider the wave growth exponents p_{ss}, q_{ss} for the self-similar core of wave spectra (fig.6). The peak frequency is growing faster than the mean frequency while the energy of the self-similar core is growing slower than the full wave energy, i.e. the non-self-similar fraction of wind-wave field can affect essentially wave growth features.

5 Discussion. A Composite Model of Wind-Wave Balance and Predictability of Wind-Wave Spectra

In this paper we showed that the self-similar solutions of the Hasselmann equation give a good approximation to the observed wind-wave spectra and parameters of wind-wave growth. These approximate solutions do not take into account details of wave input but depend on integral properties of this input. The asymptotic procedure that leads to these solutions implies a splitting of the wind-wave

balance into two parts. First, the "conservative" Hasselmann equation with no generation or dissipation terms describes a family of spectral shapes

$$\frac{\mathrm{d}N_k}{\mathrm{d}t} = S_{nl} \tag{22}$$

The parameters of the particular solution of the family is specified by the equation of integral balance of wave action (energy)

$$\langle \frac{\mathrm{d}N_k}{\mathrm{d}t} \rangle = \langle S_{in} + S_{diss} \rangle \tag{23}$$

In the consideration presented above these parameters are nothing but exponents of temporal growth of total wave action (energy). It should be stressed that the composite model is valid not for all waves but for those only which evolution is governed predominantly by non-linear transfer. Strictly speaking, the model is valid for a self-similar "core" of the solutions of the Hasselmann equation.

A key result of the present study is: the self-similar forms of wave spectra given by (22) depend very slightly on the integral balance (23). Thus, the quasi-universal spectra can be characterized effectively by their peak positions and magnitudes. This note becomes very important for non-self-similar background of wind-wave spectra. This background is beyond the composite model (22, 23). It depends on details of wind-wave balance and can affect essentially the integral energy and mean frequency. Thus, the prediction of the background behaviour is less reliable than one of the self-similar core. At the same time, the mean frequency and the total energy that characterize this background are easier to be measured in the ocean than the spectral peak properties.

As it was pointed out in Introduction, occurrence of rogue waves is likely associated with certain stages of wind-wave development. In our opinion, the analysis of wind-wave state in terms of the concept of self-similarity presented above can help in more adequate description of the wind-wave state in the context of rogue wave dynamics.

The research was conducted under US Army Corps of Engineers grants W912HZ-04-P-0172 and DACW42-03-C-0019, INTAS grant 01-234, ONR grant N00014-03-1-0648, Russian Foundation for Basic Research 02-05-6514, 04-05-64784 and the Russian Academy Program "Nonlinear Dynamics". S.I. Badulin acknowledges support of NATO under the linkage grant EST.CLG.978941.

References

1. Babanin, A.N. & Soloviev, Yu.P: Field investigation of transformation of the wind wave frequency spectrum with fetch and the stage of development, Journ.Phys. Oceanogr. **28** (1998) 563–576
2. Badulin, S., Pushkarev, A., Resio, D., Zakharov, V.: Direct and inverse cascade of energy, momentum and wave action in wind-driven sea. 7th International workshop on wave hindcasting and forecasting. Banff, October 2002, (2002) 92–103

3. Badulin, S., Pushkarev, A., Resio, D., Zakharov, V.: Self-similarity of wind-driven sea. Submitted to J. Fluid Mech. (2005)
4. Battjes, J.A., Zitman, T.J. & Holthuijsen, L.H.: A reanalysis of the spectra observed in JONSWAP. J.Phys.Oceanogr. **17** (1987) 1288–1295
5. Donelan, M.A., Hamilton J., Hui W.H.: Directional spectra of wind-generated waves. Phil.Trans.Roy.Soc.Lond. **A315** (1985) 509–562
6. Donelan, M.A. & Pierson-jr., W.J.: Radar scattering and equilibrium ranges in wind-generated waves with application to scatterometry, Journ.Geoph.Res. **92**, C5 (1987) 4971–5029.
7. Gunson, J., Holt, M.: Diagnostics for rogue wave development from spectral wave model hindcasts. Geophysical Research Abstracts **4** (2002) EGS02-A-05665
8. Hasselmann, K.: On the nonlinear energy transfer in a gravity wave spectrum. Part 1, J.Fluid Mech. **12** (1962) 481-500
9. Hasselmann, K.: On the nonlinear energy transfer in a gravity wave spectrum. Parts 2 and 3. J.Fluid Mech. **15** (1963) 273–281; 385-398
10. Hasselmann, K., Barnett, T.P., Bouws, E., Carlson, H., Cartwright, D.E., Enke, K., Ewing, J.A., Gienapp, H., Hasselmann, D.E., Kruseman, P., Meerburg, A., Muller, P., Olbers, D.J., Richter, K.,Sell, W. & Walden, H.: Measurements of wind-wave growth and swell decay during the Joint North Sea Wave Project (JONSWAP), Dtsch.Hydrogh.Z.Suppl. **12** A8 (1973)
11. Hsiao, S.V. & Shemdin, O.H.: Measurements of wind velocity and pressure with a wave follower during MARSEN. J.Geoph.Res. **88**, C14 (1983) 9841–9849
12. Holt, M., Fullerton, G., Li, J.-G.: Forecasting sea state with a spectral wave model. Rogue Waves 2004 Brest, 20-22 October 2004
13. Osborne, A. R., Onorato, M. & Serio, M.: The nonlinear dynamics of rogue waves and holes in deep water gravity wave trains. Phys. Lett. A **275** (2000) 386–393
14. Plant, W.J.: A relationship between wind stress and wave slope. Journ.Geoph. Res. **87**, C3, (1982) 1961–1967.
15. Pushkarev, A.N., Resio, D., Zakharov, V.E.: Weak turbulent theory of the wind-generated gravity sea waves. Physica D: Nonlinear Phenomena, **184** (2003) 29-63.
16. Resio, D. & Perrie, W.: A numerical study of nonlinear energy fluxes due to wave-wind interactions, J.Fluid.Mech. **223** (1991) 603–629
17. Snyder, R.L., Dobson, F.W., Elliot, J.A. & Long, R.B.: Array measurements of atmospheric pressure fluctuations above surface gravity waves, J.Fluid.Mech. **102** (1981) 1–59.
18. Stewart, R.W.: The air-sea momentum exchange, Boundary-Layer Meteorology **6** (1974) 151–167.
19. Toba, Y.: Local balance in the air-sea boundary processes. III. On the spectrum of wind waves, J.Oceanogr.Soc.Japan **29** (1973) 209–220.
20. Webb, D.J.: Non-linear transfers between sea waves. *Deep-Sea Research* **25** (1978) 279–298
21. Young, I.R.: Wind Generated Ocean Waves. Elsevier (1999)
22. Zakharov, V.E. & Filonenko N.N.: Energy spectrum for stochastic oscillations of the surface of a fluid, Dokl.Acad.Nauk SSSR **160** (1966) 1292–1295
23. Zakharov, V.E., Zaslavsky M.M.: The kinetic equation and Kolmogorov spectra in the weak-turbulence theory of wind waves, Izv.Atm.Ocean.Phys., **18** (1982) 747–753.
24. Zakharov, V.E.: Theoretical interpretation of fetch limited wind-driven sea observations. 7th International workshop on wave hindcasting and forecasting, Banff, October 2002, (2002) 86–92